# Application of a time-stable model order reduction scheme to an exterior vibro-acoustic finite element model

**S. van Ophem** [1,2], **O. Atak** [3], **E. Deckers** [1,2], **W. Desmet** [1,2]
[1] KU Leuven, Department of Mechanical Engineering,
Celestijnenlaan 300 B, B-3001, Heverlee, Belgium
e-mail: **Sjoerd.vanOphem@kuleuven.be**

[2] Member of Flanders Make

[3] Siemens Industry Software NV,
Interleuvenlaan 68, B-3001, Leuven, Belgium

## Abstract
Finite element analyses of vibro-acoustic systems are usually performed in the frequency domain, meaning that the obtained results cannot straightforwardly handle time-varying input signals. These limitations can be overcome by performing a time domain analysis of the finite element model. To reduce the calculation complexity needed for time integration a model order reduction technique is proposed. A time stable Krylov subspace reduction technique is derived for the coupled exterior vibro-acoustic problem case. The Sommerfeld radiation condition is taken into account by applying infinite elements on the boundary of the mesh. The application of time stable infinite elements leads to a potentially singular mass matrix. A method is developed that circumvents mass matrix inversion, which is based on a singular value decomposition. Combined with a special formulation of the system matrices, the proposed method is shown to preserve the stability of the full model. The resulting model order reduction procedure is applied on a numerical model of a loudspeaker.

## 1 Introduction

Numerical vibro-acoustic analysis is mostly used as tool for analyzing the acoustic behavior of a product before making a prototype. For most application cases, the required result is the steady state noise emission. To obtain these types of results, the analysis can be done in the frequency domain. Recently, more interest has been shown in time-domain vibro-acoustic analysis, since it gives also information about the transient part of the vibro-acoustic response. One of the reasons for this interest is that the time-domain model can be used in a signal processing context, for example vibro-acoustic control, structural health monitoring, parameter detection with Kalman filters or real-time sound auralization.

In this paper the focus is mainly on vibro-acoustic analysis in the low-frequency region of a structure radiating sound into the free field, in which the aim is to arrive at a model that can be used in a Digital Signal Processing (DSP) context for (semi-)real time analysis. Popular modeling methods in this frequency region are the Finite Element Method (FEM) [1] and the Boundary Element Method (BEM) [2]. We will focus on the FEM, since the BEM can potentially have some stability issues in the time domain [3]. Especially for applications that need to run in (semi-)real time, it is required that the models are restricted in size. On the other hand, it is required that the models are accurate. These demands are conflicting: For an accurate model many Degrees Of Freedom (DOF) are needed, but the calculation complexity can become demanding. Therefore, Model Order Reduction (MOR) has become active field of research. The goal of MOR techniques is to arrive at models of moderate size with a sufficient accuracy. Also, the system stability should be preserved in the Reduced Order Model (ROM), which is especially important in the time domain.

Multiple techniques are available for linear MOR, and they can mainly be subdivided into two groups: Krylov based projection methods and Truncated Balanced Reduction (TBR) methods. TBR methods are reported to maintain stability [4], but they are difficult to apply on medium to large scale problems, since they require the solution to a Lyapunov equation. On the other hand Krylov based subspace methods do not always preserve stability of the original model, but they can be applied on medium to large scale problems, if the full system matrices are sparse. Since the FEM is known for its sparse system matrices, we will look into Krylov based MOR. The stability of the model has to be assessed after reduction.

Since the model under consideration is a structure radiating sound into the free field, the model has to comply with the Sommerfeld radiation condition. Infinite elements have been applied at the edges for this reason. The chosen implementation of the infinite elements is the conjugated Astley-Leis formulation. This model has shape functions that are conjugates of the weighting functions. This results in system matrices that are frequency independent, making a transient analysis possible [5]. The resulting model will be formulated in a state space form, since this form can be implemented into a DSP context.

To discretize the resulting state space model as efficient as possible an explicit time integration scheme is preferred. Also, since the model will be derived in a DSP context, the step size of the integration scheme should be constant. Usually, explicit time integration schemes rely on the inversion of the mass matrix. Since the inclusion of the infinite elements into the system model might lead to a singular mass matrix, this leads to problems. In this paper a method is derived that handles this potentially singular matrix, so that the explicit inversion can be avoided. This will be done with a Singular Value Decomposition (SVD) that splits the mass matrix into a full rank matrix and a singular matrix. The method is shown to preserve the stability of the original model. A more detailed description of this method can also be found in [6].

In a final step, the continuous time state space model will be discretized with a zero order hold scheme in which exponential time integration is applied and a Tustin approximation (also known as a bilinear transform), respectively. Under the assumption that the original model is stable (and thus also the reduced model, under the assumptions described in this paper) it can be shown that the chosen integration schemes are stable, regardless of the chosen time step, thus making it feasible to use a stable, fast explicit time integration scheme. The described method is validated with a numerical simulation of a loudspeaker, in which the accuracy of the reduced model is compared to the full model.

# 2 Exterior vibro-acoustics in the time domain with the FEM

## 2.1 System division

The differential equation that describes the time domain solution of the coupled vibro-acoustic FEM is

$$M\ddot{x}(t) + C\dot{x}(t) + Kx(t) = Gu(t), \tag{1}$$

In this equation $M \in \mathbb{R}^{n\times n}$ is the mass matrix, $C \in \mathbb{R}^{n\times n}$ is the damping matrix, $K \in \mathbb{R}^{n\times n}$ is the stiffness matrix and $Gu(t) \in \mathbb{R}^n$ gives the external excitation. The vector $x \in \mathbb{R}^n$ is defined as the state vector that includes the field variables of interest. For the structural part these are the displacements and for the acoustic part this are either the pressure or the fluid velocity potential, depending on the formulation (see Sec. 2.2). The system consists of two physical domains: structural (subscript $s$) and acoustical (subscript $a$), and three numerical domains: The structural FE domain, the acoustic FE domain and the Infinite Elements (IE) domain. The coupling matrices between the acoustic and structural domain are indicated with subscript $c$. The boundary of the acoustic FE mesh and the IE mesh share DOFs, so the matrices for the FE and IE mesh are summed to arrive at the total system matrices. For example, the resulting stiffness matrix for the FE part of the acoustic model is

$$K_{a,11} = K_{a,FE} + K_{a,IE,inner}, \tag{2}$$

with $K_{a,FE}$ the stiffness matrix of the acoustic FE mesh and $K_{a,IE,inner}$ the stiffness matrix of the innermost nodes from the IE mesh. The stiffness matrix of the other IE nodes is indicated by subscript $K_{a,22}$ and the coupling between the nodes on the FE/IE boundary and the rest of the IE DOFs is given by $K_{a,12}$ and $K_{a,21}$.

### 2.2 Infinite elements in the modified Everstine formulation

The chosen implementation of for the IEs is the conjugated Astley-Leis formulation [7]. The application of this formulation leads to sparse, frequency independent system matrices that are applicable in the time domain [8]. However, these matrices are non-symmetric. The field variable that is solved for in the time domain is a time advanced pressure. In this paper we make use of the modified Everstine formulation (also called modified $u-\phi$), instead of the more commonly used $u-p$ formulation. In this formulation, $p = -\rho\dot{\phi}$, in which $\dot{\phi}$ is the fluid velocity potential and $\rho$ is the density of the fluid. This is done for stability reasons, see Ref. [10]. The modified $u - \phi$ formulation for the system under question is

$$M_{eve} = \begin{bmatrix} M_s & 0 & 0 \\ 0 & \rho M_{a,11} & \rho M_{a,12} \\ 0 & \rho M_{a,21} & \rho M_{a,22} \end{bmatrix}, \; C_{eve} = \begin{bmatrix} C_s & -\rho K_c & 0 \\ \rho K_c^T & \rho C_{a,11} & \rho C_{a,12} \\ 0 & \rho C_{a,21} & \rho C_{a,22} \end{bmatrix},$$

$$K_{eve} = \begin{bmatrix} K_s & 0 & 0 \\ 0 & \rho K_{a,11} & \rho K_{a,12} \\ 0 & \rho K_{a,21} & \rho K_{a,22} \end{bmatrix}, \; x_{eve} = \begin{bmatrix} u \\ \phi_{FE} \\ \phi_{IE} \end{bmatrix}, \; F_{eve} = \begin{bmatrix} F_s \\ -F_\phi \\ 0 \end{bmatrix}. \tag{3}$$

Here we made use of the observation that the time-advanced pressure, resulting from the IEs, can be written as a time-advanced fluid velocity potential.

## 3 Stability under congruence transform for exterior time domain vibro-acoustics

### 3.1 System formulation in descriptor form

To arrive at a system description that can easily be adapted into existing DSP algorithms, the system is written in its first order descriptor form:

$$\underbrace{\begin{bmatrix} I & 0 \\ 0 & M \end{bmatrix}}_{\text{E}} \underbrace{\begin{bmatrix} \dot{x}(t) \\ \ddot{x}(t) \end{bmatrix}}_{\dot{x}} = \underbrace{\begin{bmatrix} 0 & I \\ -K & -C \end{bmatrix}}_{\text{A}} \underbrace{\begin{bmatrix} x(t) \\ \dot{x}(t) \end{bmatrix}}_{\text{x}} + \underbrace{\begin{bmatrix} 0 \\ G \end{bmatrix}}_{\text{B}} u(t), \tag{4}$$

$$y(t) = \underbrace{\begin{bmatrix} C & 0 \end{bmatrix}}_{\text{C}} \underbrace{\begin{bmatrix} x(t) \\ \dot{x}(t) \end{bmatrix}}_{\text{x}} + Du(t). \tag{5}$$

Consequently, if the mass matrix is non-singular, the state space description can be acquired by inversion of the mass matrix:

$$\underbrace{\begin{bmatrix} \dot{x}(t) \\ \ddot{x}(t) \end{bmatrix}}_{\dot{x}} = \underbrace{\begin{bmatrix} 0 & I \\ -M^{-1}K & -M^{-1}C \end{bmatrix}}_{\text{A}} \underbrace{\begin{bmatrix} x(t) \\ \dot{x}(t) \end{bmatrix}}_{\text{x}} + \underbrace{\begin{bmatrix} 0 \\ M^{-1}G \end{bmatrix}}_{\text{B}} u(t), \tag{6}$$

$$y(t) = \underbrace{\begin{bmatrix} C & 0 \end{bmatrix}}_{\text{C}} \underbrace{\begin{bmatrix} x(t) \\ \dot{x}(t) \end{bmatrix}}_{\text{x}} + Du(t). \tag{7}$$

However, the described combined FE/IE formulation is possibly singular [7]. In Sec. 4 we will give a procedure for a transformation without the inversion of the mass matrix.

## 3.2 Stability requirements of singular descriptor system, resulting from a coupled FE/IE mesh

The descriptor system should be stable in the time domain. This means that the real part of the eigenvalues resulting from the generalized eigenvalue problem $(E, A)$ should be smaller than zero [9]. The eigenvalue distribution is dependent on the definiteness properties of the mass, damping and stiffness matrices. Since the matrices resulting from the IE model are non-symmetric we will use the following description for positive definiteness: Suppose the we have an non-symmetric matrix $A \in \mathbb{R}^{n\times n}$. The matrix is defined positive definite if

$$\mathfrak{Re}\{x^T A x\} > 0,\ \forall x \in \mathbb{R}^n. \tag{8}$$

This will be notated as follows: $A > 0$. For a negative (semi-) definite matrix a similar description will be used ($A < 0$). It is shown in [6] that a descriptor system is stable if $E \leq 0$ and $A > 0$. Under these conditions all the eigenvalues are either smaller than zero or infinite. The infinite eigenvalues appear due to the algebraic conditions in the system matrices and do not pose stability problems. It has been shown in [6] that for the system under consideration this leads to stability if $M \geq 0$, $K \geq 0$ and $C \geq 0$.

## 3.3 Stability under congruence transform

To arrive at the reduced order models, we apply a one-sided projection with a congruence transform. This congruence transform is done on the original system matrices, as follows:

$$\begin{aligned} M_r &= V^T M V, \\ K_r &= V^T K V, \\ C_r &= V^T C V. \end{aligned} \tag{9}$$

This equals the following reduced basis for the full state space model [13]:

$$V_{tot} = \begin{bmatrix} V & 0 \\ 0 & V \end{bmatrix}. \tag{10}$$

As has already been indicated in [10] and [6] the introduction of the coupling matrix can have an effect on the stability. Here the modified Everstine formulation is beneficial, because it leads to a cancellation of the coupling terms, which gives the following definiteness properties for the coupled damping matrix:

$$\begin{aligned} \mathfrak{Re}\{x^T C x\} &= \begin{bmatrix} x_1^T & x_2^T & x_3^T \end{bmatrix} \begin{bmatrix} C_s & -\rho K_c & 0 \\ \rho K_c^T & \rho C_{a,11} & \rho C_{a,12} \\ 0 & \rho C_{a,21} & \rho C_{a,22} \end{bmatrix} \begin{bmatrix} x_1 \\ x_2 \\ x_3 \end{bmatrix} \\ &= x_1^T C_s x_1 + \rho \begin{bmatrix} x_2^T & x_3^T \end{bmatrix} \begin{bmatrix} C_{a,11} & C_{a,12} \\ C_{a,21} & C_{a,22} \end{bmatrix} \begin{bmatrix} x_2 \\ x_3 \end{bmatrix} \geq 0. \end{aligned} \tag{11}$$

In this formulation there is no coupling matrix present in the mass matrix and in the stiffness matrix. In the $u - p$ formulation, which is commonly used in commercial FEM codes, the coupling matrix is present in both the mass and stiffness matrix, leading to an alteration of the definiteness properties under a congruence transform, thus a possible instability.

### 3.4 Model order reduction procedure

The chosen model order reduction procedure will be applied to the whole system at once. The main advantage as compared to an approach in which the domains are split is that the resulting ROM will be of a smaller size for a comparable accuracy and that the different domains will be reduced with the same accuracy [11]. This method requires the modified $u - \phi$ formulation to preserve the stability of the system. The congruence transform that will be applied is of the following form:

$$V = \begin{bmatrix} V_s \\ V_{a,11} \\ V_{a,22} \end{bmatrix} \in \mathbb{R}^{n \times k}. \tag{12}$$

If the added mass matrix because of the addition of the infinite elements is totally zero, as can be the case for infinite elements when a spherical boundary is chosen, this means that only a part of the matrix in Eq. (12) will be used for the calculation of the reduced matrix. This can be seen as follows. Define

$$\begin{aligned} V_1 &= \begin{bmatrix} V_s \\ V_{a,11} \end{bmatrix}, \; V_2 = V_{a,22}, \\ M_{11} &= \begin{bmatrix} M_s & 0 \\ 0 & \rho M_{a,11} \end{bmatrix}, \end{aligned} \tag{13}$$

The reduced mass matrix now becomes

$$M_r = \begin{bmatrix} V_1^T & V_2^T \end{bmatrix} \begin{bmatrix} M_{11} & 0 \\ 0 & 0 \end{bmatrix} \begin{bmatrix} V_1 \\ V_2 \end{bmatrix} = V_1^T M_{11} V_1. \tag{14}$$

This equation only leads to a non-singular reduced mass matrix if $V_1$ is of full column rank. If analysis shows that this matrix is of full column rank already, a transformation to state space form can be done by inversion of the mass matrix. Otherwise inversion of the reduced mass matrix to arrive at a model in the form of Eq. (6) is not possible. To circumvent this problem an alternative procedure for arriving at the form of Eq. (6) is derived.

# 4 Transformation of the singular descriptor system form to state space form

The singular descriptor system is also called a Differential Algebraic Equation (DAE), since the system that has to be solved is a combination of differential equations and algebraic equations. The best solution strategy for DAEs is dependent on the index of the problem (the amount of times the equations with algebraic constraints need to be differentiated to arrive at a full set of differential equations of the same order). Writing out the set of the equations that describe our problem (still using the notation of Sec. 3.4), we get

$$M_{11}\ddot{x}_1 = -K_{11}x_1 - C_{11}\dot{x}_1 - K_{12}x_2 - C_{12}\dot{x}_2, \tag{15}$$
$$0 = -K_{21}x_1 - C_{21}\dot{x}_1 - K_{22}x_2 - C_{22}\dot{x}_2, \tag{16}$$

If Eq. (16) is differentiated once, a full set of ordinary second order differential equations results, so our DAE is index-1.

### 4.1 Decomposition of the singular matrix

In [12] a transformation procedure is described for transforming a descriptor system describing a DAE of index 1 to a state space format. This procedure uses a full rank decomposition of $E$:

$$E = XY^T, \tag{17}$$

where $\mathrm{rank}(E) = r$ with $r \leq n$. A possible way of applying this decomposition is to apply a Singular Value Decomposition (SVD) on the matrix E and throw away the rows and columns that fall below a chosen threshold. For more details of this method, see [6]. A new state vector will be defined as follows:

$$z(t) = Y^T x(t). \tag{18}$$

This will lead to the following state space system [12]

$$\begin{aligned} \dot{z} &= \tilde{A}z + \tilde{B}u, && (19) \\ y &= \tilde{C}z + Du, && (20) \end{aligned}$$

in which

$$\begin{aligned} \tilde{A} &= (Y^T A^{-1} X)^{-1}, \\ \tilde{B} &= \tilde{A} Y^T A^{-1} B, \\ \tilde{C} &= C A^{-1} X \tilde{A}, \\ \tilde{D} &= D - C^T A^{-1} B + \tilde{C} Y^T A^{-1} B. \end{aligned} \tag{21}$$

As has been shown in [12], the eigenvalues of this new state space model are not changed under this transformation, thus the stability of the system is not affected.

### 4.2 Preservation of the descriptor system under congruence transform

A transformation as described in Sec. 4.1 would be computationally demanding if it is applied before MOR. We briefly show that this transformation can be performed after MOR, thus eliminating the need to do an SVD on the full mass matrix. This can be shown by revealing the implicit DAE form that is still present in the reduced system equations. The states of the reduced model are related to the states of the full system by the following relation:

$$\begin{bmatrix} x_1 \\ x_2 \end{bmatrix} = \begin{bmatrix} V_1 \\ V_2 \end{bmatrix} x_r. \tag{22}$$

As has been shown in Eq. (14) the reduced mass matrix is dependent on $V_1$ only. Working out the system equations in second order form gives

$$\begin{aligned} -V_1^T M_{11} \ddot{x}_1 &= \left( \begin{bmatrix} V_1^T & V_2^T \end{bmatrix} \begin{bmatrix} K_{11} & K_{12} \\ K_{21} & K_{22} \end{bmatrix} \begin{bmatrix} V_1 \\ V_2 \end{bmatrix} \right) \begin{bmatrix} V_1 \\ V_2 \end{bmatrix} x_r + \left( \begin{bmatrix} V_1^T & V_2^T \end{bmatrix} \begin{bmatrix} C_{11} & C_{12} \\ C_{21} & C_{22} \end{bmatrix} \begin{bmatrix} V_1 \\ V_2 \end{bmatrix} \right) \begin{bmatrix} V_1 \\ V_2 \end{bmatrix} \dot{x}_r \\ &= \begin{bmatrix} V_1^T & V_2^T \end{bmatrix} \begin{bmatrix} K_{11} & K_{12} \\ K_{21} & K_{22} \end{bmatrix} \begin{bmatrix} V_1 \\ V_2 \end{bmatrix} \begin{bmatrix} x_1 \\ x_2 \end{bmatrix} + \begin{bmatrix} V_1^T & V_2^T \end{bmatrix} \begin{bmatrix} C_{11} & C_{12} \\ C_{21} & C_{22} \end{bmatrix} \begin{bmatrix} V_1 \\ V_2 \end{bmatrix} \begin{bmatrix} \dot{x}_1 \\ \dot{x}_2 \end{bmatrix}. \end{aligned} \tag{23}$$

Since a single differentiation of $x_2$ leads to a full set of second order differential equations, the index-1 form of the system is still present and therefore the decomposition technique in Sec. 4.1 is still applicable.

### 4.3 Explicit time integration

After the model is transformed to a state space form, time integration can be applied. In this paper three time integration schemes are used: A Newmark-$\beta$ scheme, which is mostly used in the FE community [1], but cannot be applied on state space systems, and two time integration schemes that can be used in state space format, namely an exponential time integration scheme and Tustin's approximation. Another difference between the Newmark-$\beta$ scheme and the other two is that Newmark-$\beta$ is an implicit time integrator instead of an explicit time integrator. The exponential time integrator is given by

$$x_d[i+1] = A_d x[i] + B_d u[i], \tag{24}$$
$$y_d[i] = C_d x[i] + D_d u[i], \tag{25}$$

in which

$$\begin{aligned} A_d &= e^{\tilde{A}T_s},\ B_d = \tilde{A}^{-1}(A_d - I)\tilde{B}, \\ C_d &= \tilde{C},\ D_d = \tilde{D},\ T_s = 1/f_s. \end{aligned} \tag{26}$$

In these equations $f_s = 1/T_s$ is the chosen sampling frequency in Hz. The Tustin approximation can be seen as a lower order approximation of the matrix exponential in Eq. (26) and uses the following discrete system matrices:

$$\begin{aligned} A_d &= (I + \frac{1}{2}\tilde{A}T_s)(I - \frac{1}{2}\tilde{A}T_s)^{-1},\ B_d = T_s/2(I - (T_s/2)\tilde{A})^{-1}\tilde{B}, \\ C_d &= \tilde{C},\ D_d = \tilde{D}. \end{aligned} \tag{27}$$

## 5 Numerical validation case: Loudspeaker

We demonstrate the described procedure with a numerical model of a loudspeaker. A CAD-drawing of the loudspeaker is shown in Fig. 1. As can be seen, the loudspeaker has a woofer, a tweeter and a bass reflex port. The woofer and the tweeter are modeled in the structural domain with an FE shell mesh and the rest of the box (including the bass reflex port) is considered rigid, thus is modeled in the acoustic domain by a rigid wall boundary condition. The woofer and tweeter are clamped and proportional damping is applied. Both the acoustic field interior and exterior of the box are modeled with finite elements within a sphere of 1 m diameter and linear elements are used. The middle of the sphere is placed in the center of the box in the point $(0.0,\ 0.15,\ -0.2)$. On the edge of the sphere infinite elements with a radial order of 6 are placed to conform to the Sommerfeld radiation condition. This leads to a total amount of 25083 DOFs for the full system. The used material properties of both the woofer and the surrounding air are given in Table 1. The electro-mechanical coupling in the voice-coil actuator has not been modeled, since it is outside of the scope of this paper, but to arrive at realistic acoustic responses one could consider to include this in the model.

### 5.1 Stability and frequency response

The effectiveness of the approach in this paper will be tested by applying a Krylov subspace reduction technique, based on the Second Order Arnoldi algorithm [13]. An $H_2$ optimal model is calculated with an iterative procedure [14] and a reduced model of 200 DOFs is chosen, which is less than 1% of the original model size. The iterative algorithm finds the optimal complex expansion points. As input a force of 1 N in

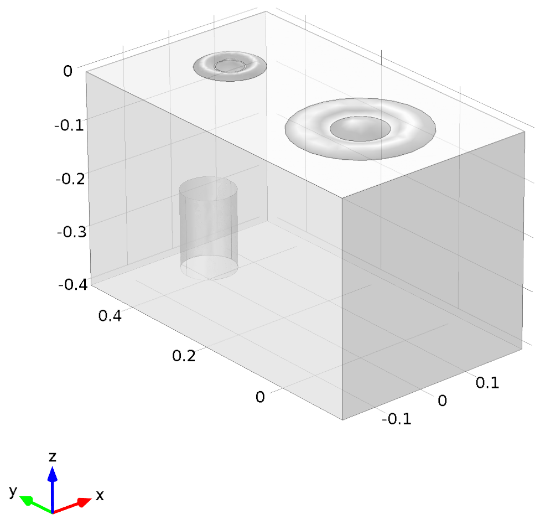


Figure 1: CAD drawing of a loudspeaker with dimensions in meters.

| Variable | Symbol | Value |
|---|---|---|
| Young's modulus | $E_s$ | $69\ \mathrm{GPa}$ |
| Possoin's ratio | $\nu_s$ | $0.3$ |
| Density (Speaker) | $\rho_s$ | $2700\ \mathrm{kg/m^3}$ |
| Thickness | $t_s$ | $0.25\ \mathrm{mm}$ |
| Proportional damping | $\alpha,\ \beta$ | $20,\ 10^{-5}$ |
| Speed of sound | $c_a$ | $340\ \mathrm{m/s}$ |
| Density (Air) | $\rho_a$ | $1.225\ \mathrm{kg/m^3}$ |

Table 1: Material properties

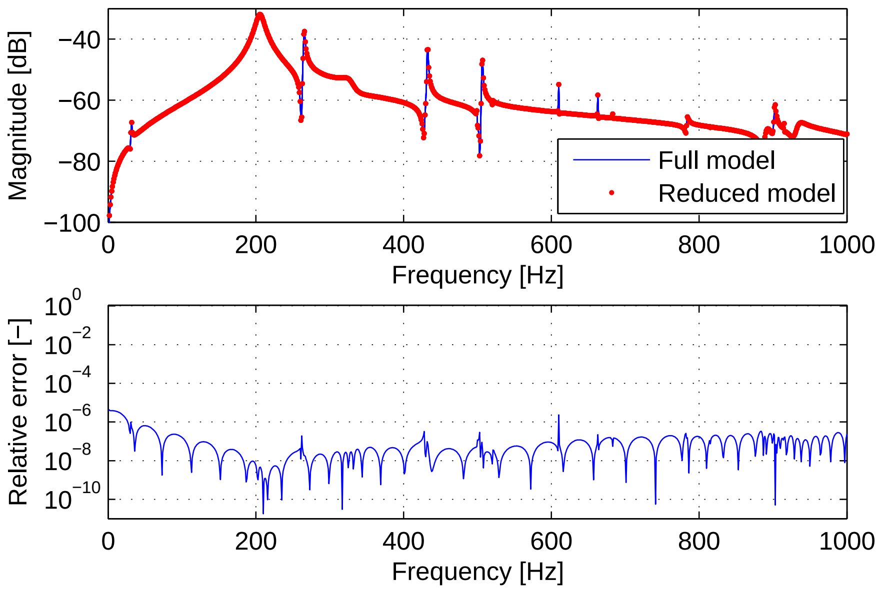


Figure 2: FRF of the full system and the reduced system (top) and relative error between the two (bottom).

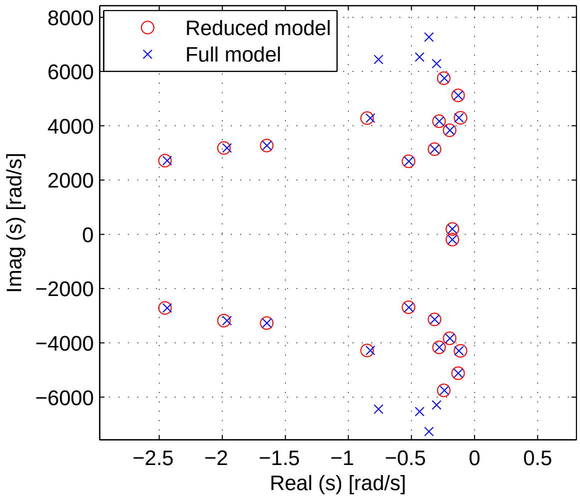


Figure 3: Eigenvalues of the full system and the reduced system.

the z-direction is applied to the woofer at the coordinate $(-0.0108,\ -0.0073,\ 0.0125)$ and as output point a coordinate in the acoustic field above the woofer is chosen: $(0.0849,\ -0.07,\ 0.0173)$. On the top of Fig. 2 a comparison is made between the Frequency Response Function (FRF) of the full system and the FRF of the reduced system and on the bottom of the figure the relative error is plotted. It can be seen that the relative error is around $10^{-7}$ in the frequency response until 1000 Hz, with the exception of the lowest frequencies. Since the response of the FRF gives very low amplitudes here, the influence of this increased error will be minimal.

The stability preservation is checked by comparing the eigenvalues between the full system and the reduced system. This is done before shifting to the discrete time domain, since a discretization maps the coordinates from the Laplace domain to the $z$-domain, making a direct comparison difficult. The result for the ROM can be seen in Fig. 3. This results are acquired after doing the transformation to state space format. It can be seen that the eigenvalues until approximately 1000 Hz are matched, which means that the model would be accurate until 1000 Hz. This is in accordance with Fig. 2.

Also the accuracy of the frequency response after discretization of the system matrices is compared. In Fig. 4 the FRF of the reduced system in continuous form, the reduced system with discretized matrices from the two discretization schemes are compared for a sampling frequency of 5000 Hz. It can be seen that the difference in FRFs between the Tustin approximation and the continuous time FRF is quite large. Some of the resonance peaks have shifted and this behavior gets worse for higher frequencies. This is a well known phenomenon of the Tustin approximation and can be reduced by pre-warping the continuous transfer function before discretization [15]. The exponential integrator has the resonance peaks at the correct positions and shows only a small difference in amplitude for higher frequencies, as compared to the continuous time FRF.

## 5.2 Time domain response

For the transient time domain response calculation a bandlimited white noise input signal is chosen in the frequency band for which the ROM is accurate. This is done by simply filtering a white noise signal with a low-pass Finite Impulse Response (FIR) filter, which is designed to have a pass-band until 950 Hz, and using the resulting signal as input to the state space model that is acquired by the procedure described above. This signal is shown in Fig. 5.

A direct comparison between the full model and the reduced model for the exponential time integration scheme is not possible, because the computational time and memory required for calculating the matrix

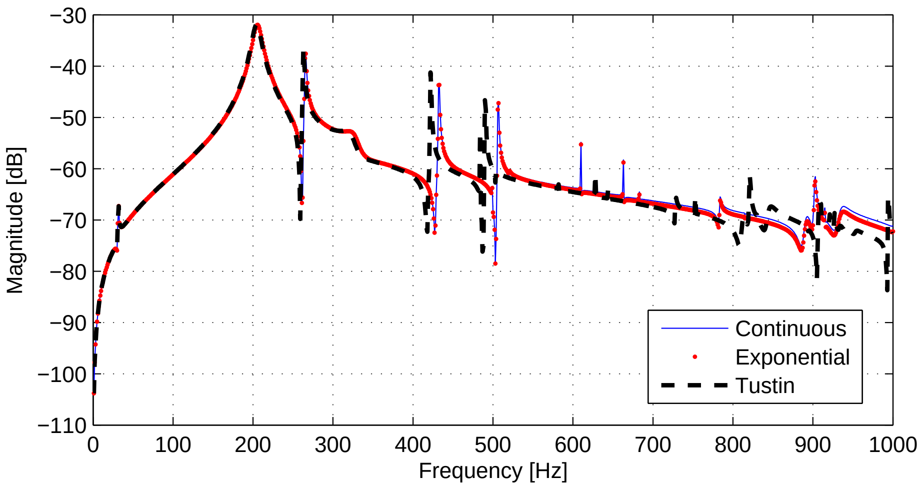


Figure 4: Comparison of the reduced model FRFs of the continous system (blue line), the Exponential system (red dots), and the Tustin approximation (black dash).

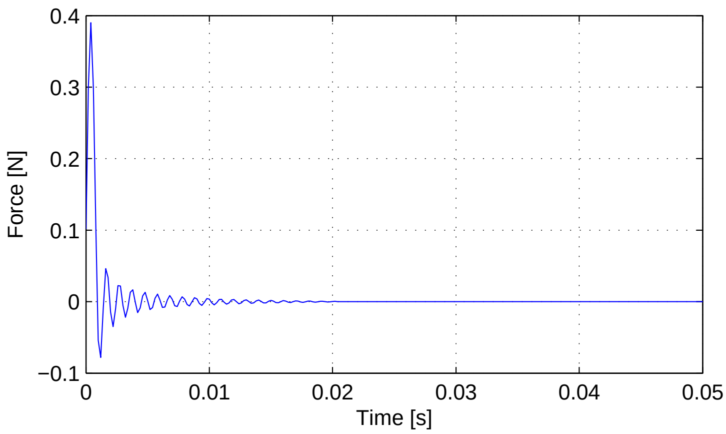


Figure 5: Input signal: A bandlimited impulsive input signal.

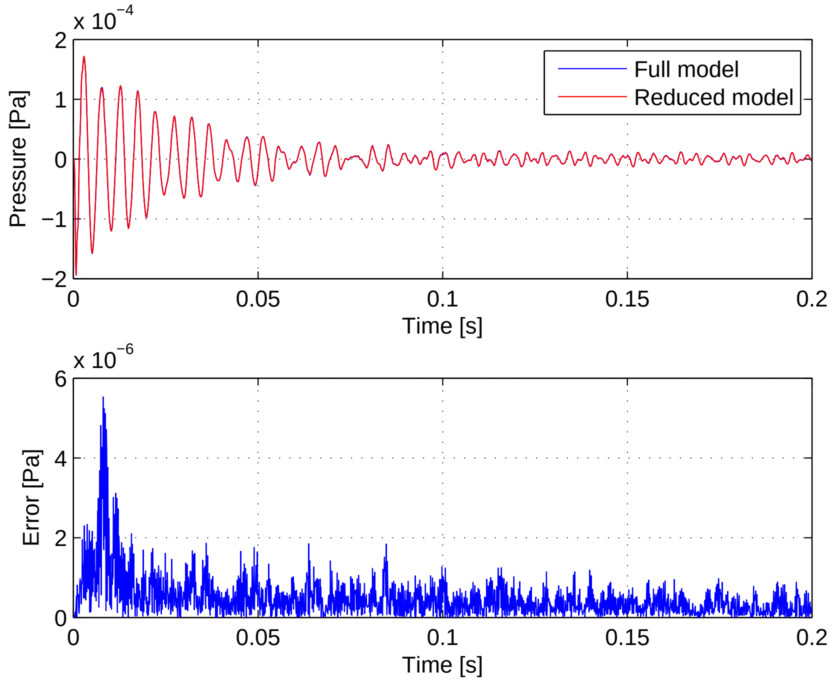


Figure 6: Time domain response of the full model and the reduced model with a Newmark-$\beta$ integrator (top) and absolute error (bottom).

exponential of the full $A$-matrix is too high. Therefore we will compare the full model and the reduced model with a Newmark-$\beta$ integration scheme, before switching our attention to the exponential integrator. The response due to the band-limited white noise signal is shown in Fig. 6 for both cases, with the error plotted in the bottom part of the figure. The Newmark scheme uses an average acceleration assumption ($\gamma = 1/2$, $\beta = 1/4$) which means that the scheme is unconditionally stable.

It can be seen that the two curves are matching almost perfectly and that the ROM preserves stability. Therefore, it can be concluded that the ROM is accurate in the time domain.

The second comparison we make is between the reduced model discretized with Newmark-$\beta$ and the discretized model with Tustin. It can be seen in Fig. 7 that the two responses are quite close. Finally, the reduced Newmark scheme is compared to the exponential time integrator, see Fig. 8. It can be seen that apparently the exponential scheme gives a higher deviation from the Newmark-$\beta$ scheme. Earlier analysis in the frequency domain showed that the exponential scheme gives more accurate frequency domain results and that the Tustin model needs pre-warping to give a better response. It seems that the Newmark-$\beta$ scheme suffers from the same problem. Therefore, the exponential integrator would be the preffered integrator for DSP applications.

When the choice of an integrator is made, the ROM can be used to calculate the pressure and displacement in every nodal point as function of time (plus in between the nodes, when the shape functions are taken into account). An example of the pressure distribution at $t = 0.0112$ s for an sinusoidal input signal at 205 Hz is shown in Fig. 9.

## 6 Conclusion

A methodology has been derived to apply model order reduction on time domain vibro-acoustic finite element models with exterior sound radiation. Furthermore, it is proved that this method preserves time stability

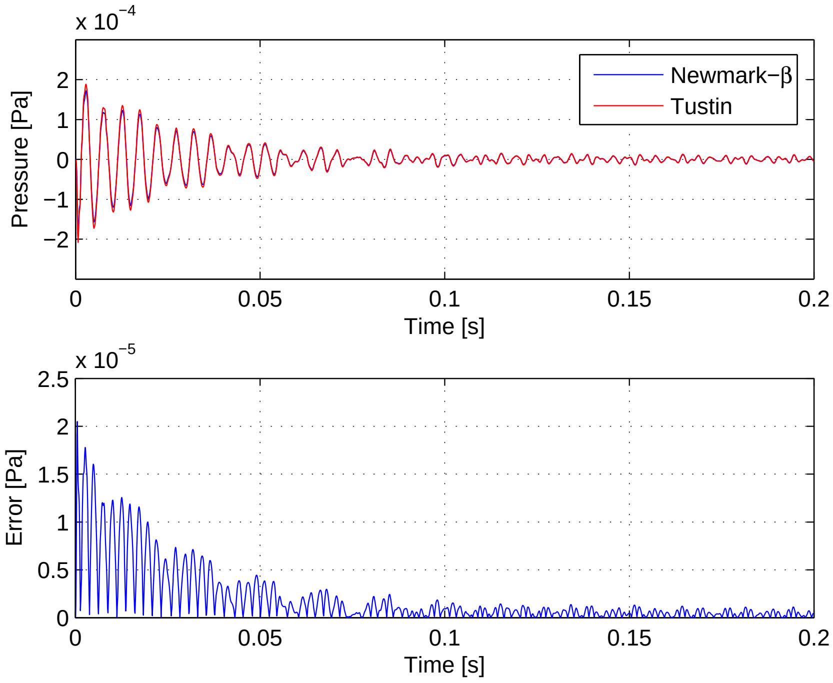


Figure 7: Time domain response of the reduced Newmark model and the reduced Tustin model (top) and absolute error (bottom).

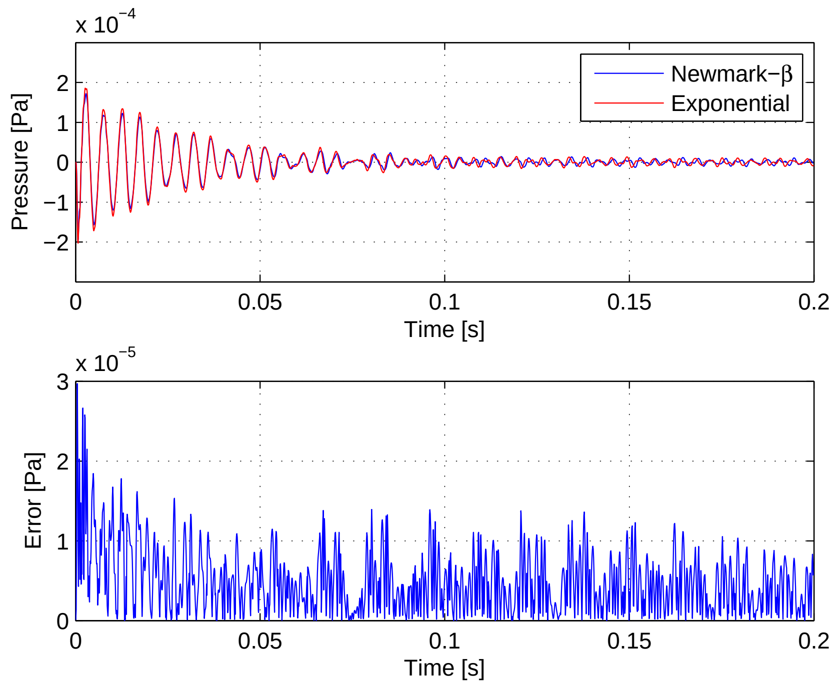


Figure 8: Time domain response of the reduced Newmark model and the reduced exponential model (top) and absolute error (bottom).

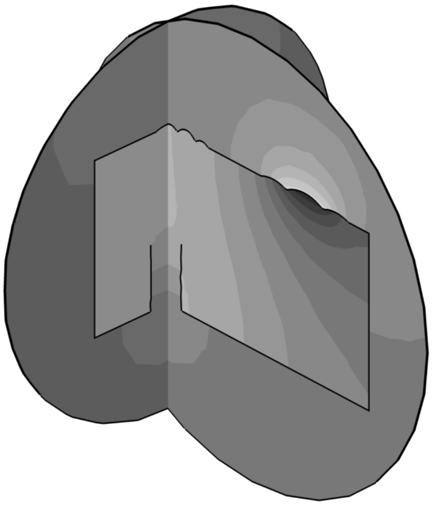

Figure 9: Pressure distribution due to sinusoidal excitation at $205\ Hz$ after $0.0122\ s$.

of the full model. The model order reduction procedure is done by a one sided projection with a congruence transform. To account for the Sommerfeld radiation condition infinite elements are added at the outer domain of the finite element mesh. The chosen implementation of the infinite elements is the conjugated Astley-Leis formulation.

It is shown that for a modified version of the Everstine formulation stability of the fully coupled system is preserved under a congruence transform. As a next step the model is transformed to a state space format, so that it can be used in a digital signal processing context. Since under a congruence transform the mass matrix can still be singular, inversion of the mass matrix is not always possible. Therefore a decomposition of the $E$-matrix, performed by a singular value decomposition on the mass matrix is performed, leading to a non-singular state space description. The resulting state space model can be discretized by an exponential time integrator or bilinear transform, leading to an explicit time integration scheme that also preserves stability.

Finally, the method is validated by a numerical vibro-acoustic simulation of a loudspeaker radiating into the free field. The accuracy of the reduced order model is assessed both in the time and frequency domain and the stability is checked by doing an eigenvalue analysis. The method is found to preserve the stability of the model and give an accurate model in the range that the FE-mesh is valid, while only using a fraction of the full system DOFs. The exponential time integrator is shown to be the most accurate of the discretization schemes described in this paper.

## Acknowledgements

The research of S. van Ophem is funded by an Early Stage Researcher grant within the European Project ANTARES Marie Curie Initial Training Network (GA 606817). The research of E. Deckers is funded by a grant from the Fund for Scientific Research Flanders (F.W.O). The Research Fund KU Leuven is gratefully acknowledged for its support. The research was partially supported by Flanders Make, the strategic research center for the manufacturing industry.

## References

[1] R. D. Cook, D. S. Malkus, M. E. Plesha, R. J. Witt, *Concepts and Applications of Finite Element Analysis (fourth edition)*, Wiley, Madison (2002).

[2] O. von Estorff, *Boundary Elements in Acoustics: Advances and Applications*, WITpress, (2000).

[3] A. A. Ergin, B. Shanker, E. Michielssen, *Analysis of transient wave scattering from rigid bodies using a Burton Miller approach*, The Journal of the Acoustical Society of America, Vol. 106, No. 5, (1999), pp. 2396-2404.

[4] B. Moore, *Principal component analysis in linear systems: Controllability, observability, and model reduction*, IEEE Transactions on Automatic Control, Vol. 26, No. 1, (1981), pp. 17-32.

[5] E. J. Grimme, *Krylov Projection Methods for Model Reduction*, University of Illinois, Illinois (1997).

[6] S. van Ophem, O. Atak, E. Deckers, W. Desmet, *Stable model order reduction for time-domain exterior vibro-acoustic finite element simulations*, Manuscript submitted for publication in: Computer Methods in Applied Mechanics and Engineering (2016).

[7] R. J. Astley, G. J. Macaulay, J.P. Coyette, L. Cremers, *Three-dimensional wave-envelope elements of variable order for acoustic radiation and scattering. Part I: Formulation in the frequency domain*, The Journal of the Acoustical Society of America, Vol. 103, No. 1, (1998), pp. 39-63.

[8] R. J. Astley, G. J. Macaulay, J.P. Coyette, L. Cremers, *Three-dimensional wave-envelope elements of variable order for acoustic radiation and scattering. Part II: Formulation in the time domain*, The Journal of the Acoustical Society of America, Vol. 103, No. 1, (1998), pp. 64-72.

[9] D. Guan, *Analysis and Design of Linear Descriptor Systems*, Springer-Verlag, New York (2010).

[10] A. van de Walle, F. Naets, E. Deckers, W. Desmet, *Stability-preserving model-order reduction for time-domain simulation of vibro-acoustic FE models*, International Journal for Numerical Methods in Engineering, Forthcoming (2016).

[11] R. W. Freund, *Model Order Reduction: Theory, Research Aspects and Applications*, Springer-Verlag, Heidelberg (2008).

[12] S. S. K. Sajja, *Stability results for constrained dynamical systems*, National University of Ireland Maynooth (2012).

[13] Z. Bai, Y. Su, *SOAR: A Second-order Arnoldi Method for the Solution of the Quadratic Eigenvalue Problem*, SIAM Journal on Matrix Analysis and Applications, Vol. 26, No. 3, (2005), pp. 640-659.

[14] S. Gugercin, A. C. Antoulas, C. A. Beattie, *A Rational Krylov Iteration for Optimal $H_2$ Model Reduction*, in *Proceedings of the 17th International Symposium on Mathematical Theory of Networks and Systems*, Japan (2006), pp. 1665-1667.

[15] J. G. Proakis, D. G. Manolakis, *Digital Signal Processing: Principles, Algorithms and Applications, Fourth Edition*, Pearson Prentice Hall, New Jersey (2007).